IEEE Photonics Journal
An IEEE Photonics Society Publication

Reflection and Transmission Modes in Nanohole-Array-Based Plasmonic Sensors

Volume 4, Number 1, February 2012

L. Wu, Member, IEEE
P. Bai, Member, IEEE
X. Zhou
E. P. Li, Fellow, IEEE

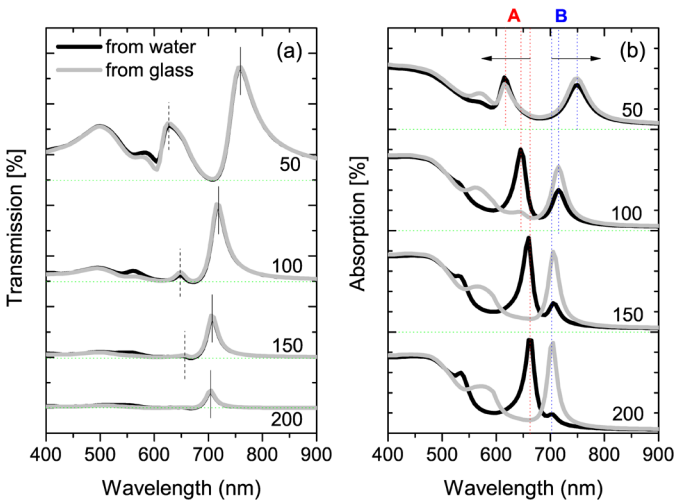

DOI: 10.1109/JPHOT.2011.2177652
1943-0655/$26.00 ©2011 IEEE

Reflection and Transmission Modes in Nanohole-Array-Based Plasmonic Sensors

L. Wu,[1] *Member, IEEE*, P. Bai,[1] *Member, IEEE*, X. Zhou,[2] and E. P. Li,[1] *Fellow, IEEE*

[1]Electronics and Photonics Department, Institute of High Performance Computing, Agency for Science, Technology, and Research (A*STAR), Singapore 138632
[2]Materials Analysis and Characterization Group, Institute of Materials Research and Engineering, Agency for Science, Technology, and Research (A*STAR), Singapore 117602

DOI: 10.1109/JPHOT.2011.2177652

Manuscript received October 9, 2011; revised November 11, 2011; accepted November 18, 2011. Date of publication November 29, 2011; date of current version December 23, 2011. This work was supported by the Singapore A*STAR-SERC integrated nano-photo-bio interface (iNPBi) thematic strategic research program (TSRP) Grant 102 152 0014. Corresponding author: L. Wu (e-mail: wul@ihpc.a-star.edu.sg).

Abstract: Reflection and transmission modes are studied in a surface plasmon resonance (SPR) sensor, where a nanohole-array-patterned gold film is deposited on a glass substrate, and the analyte in an aqueous medium is bound onto the patterned gold film. The reflection (transmission) mode means that light illuminates the structure from the analyte (substrate) side, and the detection is fixed at the analyte side. The two modes are studied by calculating absorption (and transmission) spectra and optical field distributions of the sensor. This study shows that both modes can excite the SPR on the analyte/gold interface, which is useful for sensing. However, the optical field distribution at the resonant wavelength is different for the two modes, and the effect is dependent on the gold film thickness. Comparing the sensing performance, the reflection mode gives larger resonant optical field enhancements (32 as compared with 22), but the transmission mode uses much thinner gold films (60 nm as compared with 150 nm). The optical power flow is analyzed to understand the fundamental difference between the two modes. These findings are particularly useful to guide the design of metallic nanostructure-based plasmonic sensing systems.

Index Terms: Nanohole arrays, plasmonics, biosensors.

1. Introduction

When light illuminates on a metal film patterned with an array of nanoholes, strongly enhanced transmission at selected wavelengths, i.e., the extraordinary optical transmission (EOT), has been observed [1]–[6]. This knowledge is opening up exciting new opportunities in applications in the field of sensing and spectroscopy [7]–[15]. More specifically, this EOT property of the nanohole arrays can be used in surface plasmon fluorescence spectroscopy (SPFS) [16]–[18] for the detection of a clinically relevant sample, i.e., the analyte, which is bound onto the nanohole array. The reason of using nanohole array EOT for SPFS detection is because some of the EOT transmission peaks are due to surface plasmon resonance (SPR). The strong electromagnetic field enhancements associated with SPR can be used to excite the fluorescent molecules that are attached to the analytes. In this sense, each fluorescent molecule acts as an amplifier, and more bound analytes on the nanohole array means more amplifiers. In this way, the detected intensity of the fluorescence signal represents the concentration of the analyte.

Conventional SPFS uses the Kretschmann coupling prism method to excite the surface plasmon polariton (SPP) at the planar surface of a metal film [16], [17], which is bulky (due to the prism), costly (due to the helium-neon laser) and also requires precise control of the incident angle. Besides, the wavelength of the excited SPP (i.e., 438 nm) does not match the fluorescent molecules' excitation wavelength (i.e., 647 nm) [16]. On the other hand, the nanohole-array-based SPFS allows us to remove the bulky prism, to use white light or bright LED as light source, to illuminate the light source at normal incident angle, and to tune its resonant wavelength [18]. Therefore, it will be more compact, cost-effective, and potentially achieving lower detection limit.

To implement the SPFS with the nanohole arrays, a metal film is deposited and patterned on a glass substrate, and the analyte in an aqueous medium (e.g., buffer, human urine, or human serum) is bound onto the surface of the metal film. To excite the SPR of such a structure, the light source could be put at the analyte or substrate side, but the detection should be fixed at the analyte side to capture the fluorescence signal. In this manner, the sensor can be operated in either reflection or transmission mode.

For both modes the fluorescence intensity should be detected in a dark background (i.e., to ensure that the illumination light will not be detected by the photodetector). This leads to different sensor system configurations for the two modes. In reflection mode, a dark-field lens can be positioned at the analyte side to illuminate the light annularly at an oblique angle and collect the fluorescence at the center. In transmission mode, a cardioid condenser can be adopted at the substrate side to illuminate at a large oblique angle so that the illuminating light will not be collected by the detector having a small numerical aperture. In this way, the transmission mode provides a larger space (at the analyte side) for adding optical filters to eliminate the unwanted scattered light and increase the signal-to-noise ratio. However, the surface plasmon excitation is usually stronger at the side of the light incidence, and therefore, the fluorescence molecules could be more strongly excited in the reflection mode.

Based on these pros and cons, it is difficult to decide which mode shall be adopted in the engineering design of a sensor as the system configuration, implementation complexity, sensing resolution, and cost will be quite different. We are therefore motivated to make further efforts to carefully study the two modes from the fundamentals, with the objective to see what kind of SPR will be excited, how the resonant optical field enhancement is distributed, and how these are impacted by the two illumination directions and the gold film thickness. We hope that the additional information acquired from this study would provide more insight to determine which illumination mode is more preferable for particular applications.

2. Method of Analysis

Our study is based on an ideal water–gold–glass structure, where a nanohole array is patterned in a gold film that is deposited on a glass substrate and the array is assumed in the water environment. For simplicity and generality, we do not include the adhesion layer, the analyte binding layer, and the analyte layer in our structure, and we assume that our nanohole array structure is ideal (i.e., the possible nonuniformity, fabrication error bar, nonideal hole shape, slant sidewall, rounded corner etc., which may appear in real experiments are all ignored). This is justified, because our simulation results suggest that the inclusion of these effects only slightly changes the spectral locations of the structure's resonances and the relative optical field enhancement.

To simulate the optical response of a structure to a white light illumination, we use the finite element method (time-harmonic analysis) to solve the full set of 3-D Maxwell's equations for transmission, reflection, absorption spectra, and optical field distributions [18]. The time-harmonic analysis assumes that all variations in time occur as sinusoidal signals, and the problem is formulated as a stationary problem with complex-valued solutions. The complex value represents both the amplitude and the phase of the field, while the frequency is specified as a predefined variable. In this way, we can directly use (without any model fitting) the measured frequency-dependent dielectric function of gold from Palik handbook [19] and assign the refractive index of 1.49 (1.33) to the glass (water). To validate our model, we show one comparison with experimental data in Fig. 1, where a nanohole array

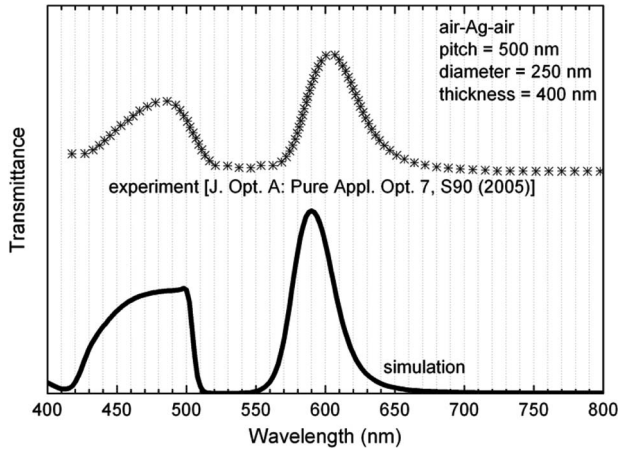

Fig. 1. Simulated and measured transmission spectra for a nanohole array structure (500-nm-pitch and 250-nm-diameter) fabricated in a 400-nm-thick silver film suspended in air.

(500-nm-pitch and 250-nm-diameter) is fabricated in a 400-nm-thick silver film suspended in air. The great agreement gives us sufficient confidence to apply our model to design the nanohole-array-based plasmonic sensing substrate. Besides, it has also been demonstrated [18] that the absorption spectrum carries more information and is more directly correlated to the SPR, and the optical field distribution is important to assist us in finding the physical location of the SPR.

A square lattice nanohole array is fully characterized by three parameters: the array pitch, the hole diameter, and the gold film thickness. However, in the present study, our focus is on which side of the structure should be illuminated, and we find that the only essential parameter is the thickness of the gold film (i.e., the spacing between the glass/gold and water/gold interfaces which influences the optical power distributions along the light propagating direction). The other two parameters (pitch and diameter) are more to tune the spectral location of the resonance and to adjust the optical power distributions in the planes perpendicular to light propagating direction [18]. Assuming the fluorescent molecules' excitation wavelength is 647 nm in a SPFS experiment, we have optimized our nanohole array structure to have a 400-nm-pitch and a 150-nm-hole-diameter. Then, various gold film thicknesses will be examined carefully in both reflection and transmission modes.

Fig. 2 shows transmission and absorption spectra for nanohole arrays milled in gold films of thickness 50, 100, 150, and 200 nm. In the calculations, two illumination conditions are considered: from the water (black) or glass (gray) side. It is clear from Fig. 2(a) that the transmission spectrum varies with the gold film thickness for both reflection and transmission modes. As the film thickness is reduced from 200 nm to 50 nm gradually, the transmission peak around 700 nm has a red-shift and becomes more prominent, and the other transmission peak around 650 nm appears gradually and experiences a blue-shift. More importantly, however, we observe that the transmission spectrum is invariant no matter which side of the structure is illuminated. This finding is consistent with the experimental observations in the pioneer paper "extraordinary optical transmission through sub-wavelength hole arrays" by Ebbesen [1] and agrees with the classical Helmholtz reciprocity principle [20], which also demonstrates the reliability of our calculations. Still, there are some unpleasant mismatches between the two illumination conditions in Fig. 2(a) (up to 3.43% for the 50-nm gold film), especially in the region from 550 nm to 600 nm, which are due to numerical errors.

On the other hand, the absorption spectrum shown in Fig. 2(b) gives us different but more interesting information. The illumination condition does influence the absorption spectrum. There are two major absorption peaks: peaks A are at about 610–660 nm, and peaks B about 700–750 nm. For a thicker film thickness like 200 nm, the peak A is dominant if illuminating from the water side, whereas the peak B is dominant if illuminating from the glass side. However, for a thinner film thickness

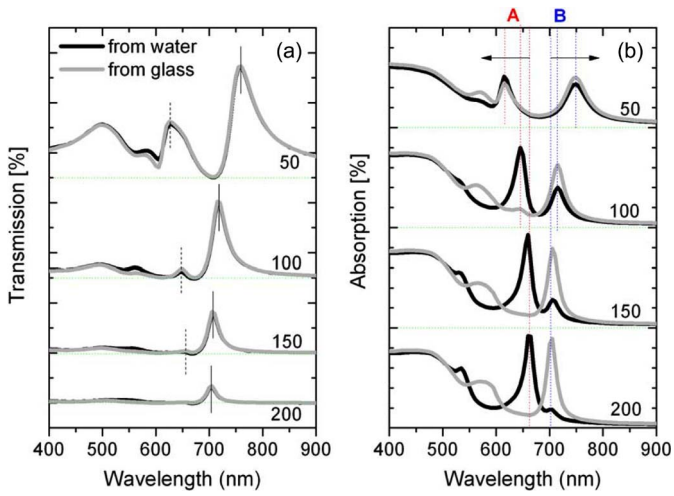

Fig. 2. Spectra of (a) transmission and (b) absorption for nanohole arrays (400-nm-pitch and 150-nm-diameter) which are milled in gold films of thickness 50, 100, 150, and 200 nm, where the light illuminates the structures from the water (black) or glass (gray) side.

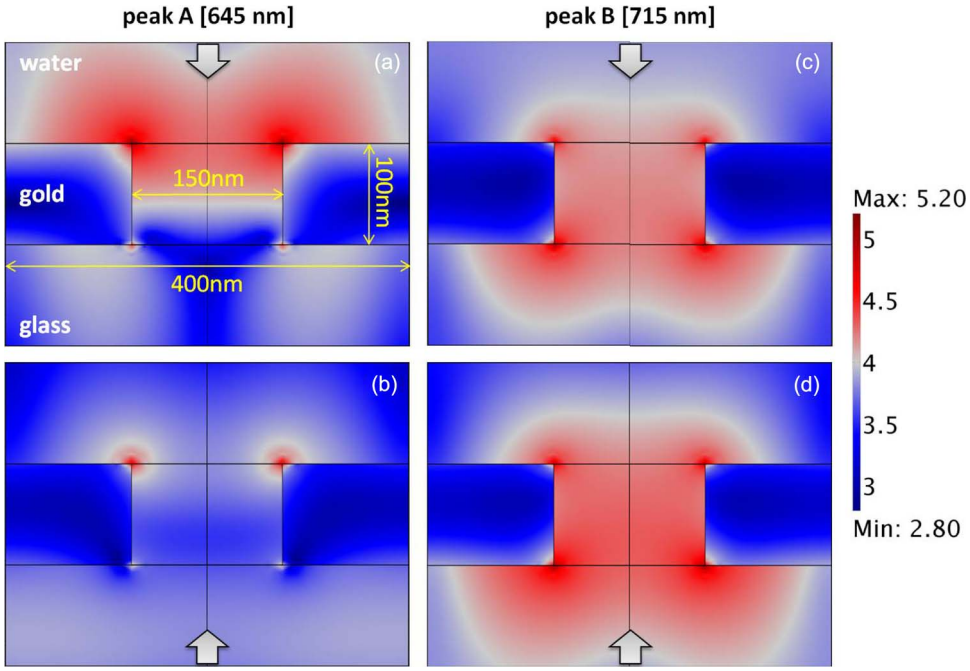

Fig. 3. Cross-sectional view of the optical field distributions (V/m) (in log-scale) for two cases where the light illuminates the sample from the water [(a) and (c)] or glass [(b) and (d)] side at two peak wavelengths: peak A [(a) and (b)] or B [(c) and (d)]. The hole array under analysis is composed of many 150-nm-diameter and 100-nm-depth holes arranged with 400-nm-pitch.

such as 50 nm, both peak A and B are present no matter which side is illuminated. These interesting observations seem to suggest that there may be some physics behind.

To gain more details behind the peak A and B in the absorption spectrum, we pick up the 100-nm-thick hole array and show its optical field distributions (V/m) (in log-scale) in Fig. 3 (cross-sectional view). Among the four plots, (a) and (c) represent the case that the sample is illuminated from the water side, and (b) and (d) represent the other case. Moreover, (a) and (b) shows the optical fields

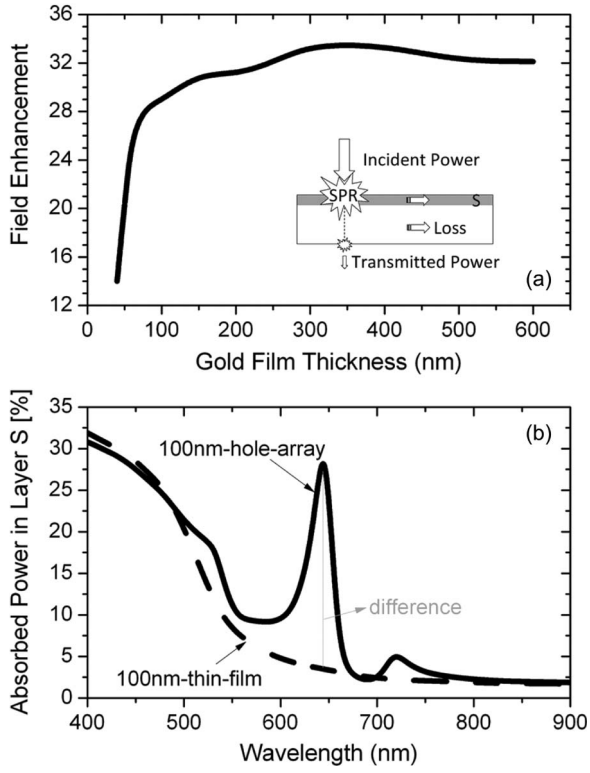

Fig. 4. Illuminating from water side, (a) the peak A optical field enhancement γ at the rim of holes of the water/gold interface is shown as a function of gold film thickness. The inset shows the optical power flow when light is illuminating from water side. (b) Absorbed optical power in the layer S (i.e., the 10-nm-gold-surface-layer near the water/gold interface), which is represented by the hatched area in the inset of (a), for a 100-nm-thick nanohole array (solid line) and a 100-nm-thick thin film (dashed line).

at peak A (resonant wavelength 645 nm), and (c) and (d) are at peak B (715 nm). We find that, the plots corresponding to peak A always show the evidence of the SPR at the water/gold interface. The signal in (a) is stronger than that in (b), which means that illuminating from the water side lead to stronger SPR at water/gold interface. On the other hand, in Fig. 3, the plots (c) and (d), corresponding to peak B, exhibit the SPR at primarily the glass/gold interface and secondarily the water/gold interface, because the signal at the glass/gold interface is stronger. This is true no matter which side is illuminated. However, the signal in (d) is slightly stronger than that in (c).

Knowing that the peak A correlates the SPR at the water/gold interface and the peak B correlates the SPR at the glass/gold interface, we shall focus our study on the former because the analyte (attached with the fluorescent molecules) is bound at the water/gold interface. Besides, in the SPFS experiment, we need to optimize the optical fields around the fluorescent labels to excite them more efficiently. Hence, in the following studies, we will focus on the optical field enhancement $\gamma = E/E_{0x}$ at the resonant wavelength of peak A, where E_{0x} is the electric field component of the incident light wave.

3. Results and Discussions

Fig. 4(a) shows for the reflection mode the plot of optical field enhancement γ as a function of the gold film thickness, where γ is evaluated at the rim of the holes near the water/gold interface. It is found that γ increases with the film thickness rapidly before it saturates around a value of 32 with a variation of 3.5% when a critical film thickness 150 nm is reached. The mechanism behind this observation could be explained by analyzing the optical power flow, as illustrated in the inset of Fig. 4(a).

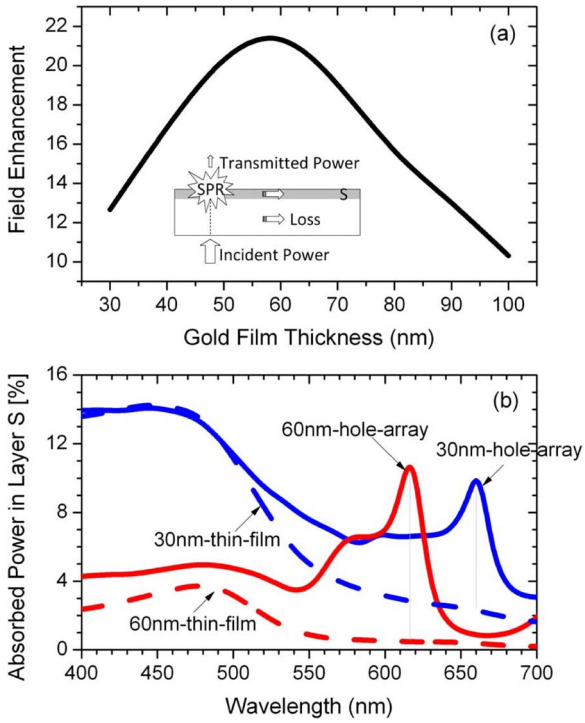

Fig. 5. Illuminating from glass side, (a) the peak A optical field enhancement γ at the rim of holes of the water/gold interface is shown as a function of gold film thickness. The inset shows the optical power flow when light is illuminating from glass side. (b) Absorbed optical power in the layer S (i.e., the 10-nm-gold-surface-layer near the water/gold interface), which is represented by the hatched area in the inset of (a), for 30, 60-nm-thick nanohole arrays (solid lines) and 30, 60-nm-thick thin films (dashed lines).

In the reflection mode, the incident optical power first excites the SPR at the water/gold interface, then passes through the bulk metal film with some optical loss which is related to the imaginary part of the metal's refractive index, and then induces some weak response at glass/gold interface before it finally transmits out. To get more information of the SPR at the water/gold interface, we specifically calculate the absorbed optical power in the 10-nm-gold-surface-layer near the water/gold interface, i.e., the layer S (hatched area) in the inset of Fig. 4(a). The absorbed optical power in the layer S should consist of the power used to excite the water/gold SPR and the optical loss in that 10 nm layer. To demonstrate this, in Fig. 4(b), we plot the absorbed power in layer S for a 100-nm-thick nanohole array and a 100-nm-thick thin film. We know that the surface-layer power absorption for the thin film structure is purely due to the optical loss. Thus, the surface-layer power absorption difference between the hole array, and the thin film is the optical power to excite the water/gold SPR, assuming the loss in their surface-layers is the same.

We did the same analysis for other thicknesses (not shown to simplify the figure), but the trend of layer S power absorption is the same as that of the total power absorption which is shown in Fig. 2(b) (black). We find that as gold film becomes thinner, the resonant peak A continues decreasing in its magnitude, while the optical loss in the incident 10-nm-surface-layer is independent of film thickness. This suggests that less optical power is used to excite the water/gold SPR as film thickness reduces. Consequently, a relatively thick film ($>$ 150 nm) is required in the reflection mode.

On the other hand, if the biosensor is operated in the transmission mode, things are different, as shown in Fig. 5(a). We observe that the optimized film thickness to maximize γ is much thinner, which is about 60 nm. In this case, the light is incident on the glass side and passes through the gold film to the water side; only part of the passed-through optical power (i.e., those have reached the S layer) is used to excite the water/gold SPR, as illustrated in the inset of Fig. 5(a). Intuitively, it is expected that an extremely thin film that is even optically transparent is desirable. Fig. 2(b) (gray)

clearly demonstrates this point, where the peak A's magnitude is increasing continuously with reduced film thickness.

However, this is only true till the film thickness is reduced to 60 nm. Beyond 60 nm, the value of optical field enhancement starts to drop down, as shown in Fig. 5(a). To find out the reason, we plot the S layer power absorption for the 60-nm-thick and 30-nm-thick hole arrays (solid lines) and thin films (dash lines) in Fig. 5(b). We find that the 30-nm-thick thin film allows more optical power to reach the 10 nm gold surface layer, as the absorbed power in the layer S is substantially increased. This is because 30 nm is very close to the skin depth of gold in the visible spectrum. However, most of the reached optical power is going to the loss in that 10 nm layer and not going to the resonant excitation of SPR, as we see that the surface-layer power absorption difference between hole array and thin film is reduced as film thickness decreases from 60 nm to 30 nm. In a word, if illuminating from the glass side, a much thinner (but $>$ skin depth) gold film must be used. From another perspective, thinner gold film is good in saving material costs. Comparing 150 nm for reflection mode and 60 nm for transmission mode, 60% gold film reduction is achieved.

Besides knowing the ideal film thickness for each mode and the mechanism behind, the magnitude of optical field enhancement γ is also important, because the amount of the relevant plasmonic optical power (i.e., square of optical field) is used to excite the fluorescent molecules. As shown in Figs. 4(a) and 5(a), γ is saturated at about 32 if illuminating from the water side, and it is maximized about 22 if illuminating from the glass side. In terms of plasmonic optical power (which is proportional to number of photons per second), the reflection mode is twice as large as the transmission mode, which could generate much stronger fluorescence signals. Fundamentally, this is because in reflection mode the incoming optical power is directly used to excite the water/gold SPR, but in transmission mode, the incoming optical power first suffers the loss and then excites the SPR.

4. Conclusion

We have presented in-depth studies on exciting the SPR of a water–gold(holes)–glass structure illuminated from either water (reflection mode) or glass side (transmission mode). Our studies show that both modes can excite the resonance at water/gold interface, which is used in SPFS. This resonance correlates different absorption spectra and optical field distributions when changing the illumination direction or the gold film thickness, due to the changed optical power flow and surface layer power absorption. In the reflection mode, thicker gold film ($>$ 150 nm) is preferred, whereas thinner film (60 nm) is necessary in the transmission mode, in order to optimize the sensing performance. The reflection mode is superior in providing larger optical field enhancements (32 as compared to 22), i.e., in terms of plasmonic optical power to generate the fluorescence signal, it is twice as large as the transmission mode. However, the transmission mode has more space to add optical filters to increase the signal-to-noise ratio in real engineering designs, and it also uses much thinner gold films (60% reduction) so that the material costs are much lower. These findings could assist people in determining the favorable illumination direction and gold film thickness in the design of the metallic nanostructure-based plasmonic sensing systems.

Acknowledgment

The authors wish to thank Prof. M. S. Tse from Nanyang Technological University for fruitful discussions on the experimental setup to implement the SPFS using the nanohole array structure.

References

[1] T. W. Ebbesen, H. J. Lezec, H. F. Ghaemi, T. Thio, and P. A. Wolff, "Extraordinary optical transmission through sub-wavelength hole arrays," *Nature*, vol. 391, no. 6668, pp. 667–669, Feb. 1998.

[2] H. F. Ghaemi, T. Thio, D. E. Grupp, T. W. Ebbesen, and H. J. Lezec, "Surface plasmons enhance optical transmission through subwavelength holes," *Phys. Rev. B, Condens. Matter*, vol. 58, no. 11, pp. 6779–6782, Sep. 1998.

[3] A. Degiron, H. J. Lezec, W. L. Barnes, and T. W. Ebbesen, "Effects of hole depth on enhanced light transmission through subwavelength hole arrays," *Appl. Phys. Lett.*, vol. 81, no. 23, pp. 4327–4329, Dec. 2002.
[4] J. Prikulis, P. Hanarp, L. Olofsson, D. Sutherland, and M. Kall, "Optical spectroscopy of nanometric holes in thin gold films," *Nano Lett.*, vol. 4, no. 6, pp. 1003–1007, 2004.
[5] C. Genet and T. W. Ebbesen, "Light in tiny holes," *Nature*, vol. 445, no. 7123, pp. 39–46, Jan. 2007.
[6] F. J. Garcia-Vidal, L. Martin-Moreno, T. W. Ebbesen, and L. Kuipers, "Light passing through subwavelength apertures," *Rev. Mod. Phys.*, vol. 82, no. 1, pp. 729–787, Mar. 2010.
[7] M. J. Levene, J. Korlach, S. W. Turner, M. Foquet, H. G. Craighead, and W. W. Webb, "Zero-mode waveguides for single-molecule analysis at high concentrations," *Science*, vol. 299, no. 5607, pp. 682–686, Jan. 2003.
[8] A. G. Brolo, R. Gordon, B. Leathem, and K. L. Kavanagh, "Surface plasmon sensor based on the enhanced light transmission through arrays of nanoholes in gold films," *Langmuir*, vol. 20, no. 12, pp. 4813–4815, Jun. 2004.
[9] A. G. Brolo, S. C. Kwok, M. G. Moffitt, R. Gordon, J. Riordon, and K. L. Kavanagh, "Enhanced fluorescence from arrays of nanoholes in a gold film," *J. Amer. Chem. Soc.*, vol. 127, no. 42, pp. 14 936–14 941, Oct. 2005.
[10] K. A. Tetz, L. Pang, and Y. Fainman, "High-resolution surface plasmon resonance sensor based on linewidth-optimized nanohole array transmittance," *Opt. Lett.*, vol. 31, no. 10, pp. 1528–1530, May 2006.
[11] G. M. Hwang, L. Pang, E. H. Mullen, and Y. Fainman, "Plasmonic sensing of biological analytes through nanoholes," *IEEE Sensors J.*, vol. 8, no. 12, pp. 2074–2079, Dec. 2008.
[12] A. A. Yanik, M. Huang, A. Artar, T. Y. Chang, and H. Altug, "Integrated nanoplasmonic–nanofluidic biosensors with targeted delivery of analytes," *Appl. Phys. Lett.*, vol. 96, no. 2, p. 021101, Jan. 2010.
[13] A. A. Yanik, M. Huang, O. Kamohara, A. Artar, T. W. Geisbert, J. H. Connor, and H. Altug, "An optofluidic nanoplasmonic biosensor for direct detection of live viruses from biological media," *Nano Lett.*, vol. 10, no. 12, pp. 4962–4969, Nov. 2010.
[14] T. Sannomiya, O. Scholder, K. Jefimovs, C. Hafner, and A. B. Dahlin, "Investigation of plasmon resonances in metal films with nanohole arrays for biosensing applications," *Small*, vol. 7, no. 12, pp. 1653–1663, Jun. 2011.
[15] M. Das, D. Hohertz, R. Nirwan, A. G. Brolo, K. L. Kavanagh, and R. Gordon, "Improved performance of nanohole surface plasmon resonance sensors by the integrated response method," *IEEE Photon. J.*, vol. 3, no. 3, pp. 441–449, Jun. 2011.
[16] F. Yu, B. Persson, S. Lofas, and W. Knoll, "Surface plasmon fluorescence immunoassay of free prostate-specific antigen in human plasma at the femtomolar level," *Anal. Chem.*, vol. 76, no. 22, pp. 6765–6770, Nov. 2004.
[17] Y. Wang, A. Brunsen, U. Jonas, J. Dostalek, and W. Knoll, "Prostate specific antigen biosensor based on long range surface plasmon-enhanced fluorescence spectroscopy and dextran hydrogel binding matrix," *Anal. Chem.*, vol. 81, no. 23, pp. 9625–9632, Dec. 2009.
[18] L. Wu, P. Bai, and E. P. Li, "Designing surface plasmon resonance of subwavelength hole arrays by studying absorption," *J. Opt. Soc. Amer. B, Opt. Phys.*, Dec. 2011.
[19] E. D. Palik, *Handbook of Optical Constants of Solids*. New York: Academic, 1998.
[20] B. Hapke, *Theory of Reflectance and Emittance Spectroscopy*. Cambridge, U.K.: Cambridge Univ. Press, 1993.